

Histone Methyltransferase G9a Promotes Invasion of Non-small Cell Lung Cancer Through Enhancing Focaladhesionkinase Activationvia NF-KB Signaling Pathway

Ting Sun

City of Hope National Medical Center

Keqiang Zhang

City of Hope National Medical Center

Rajendra P. Pangen

City of Hope National Medical Center

Wendong Li

City of Hope National Medical Center

Yong Du

General Hospital of Ningxia Medical University

Shyambabu Chaurasiya

City of Hope National Medical Center

Leonidas Arvanitis

City of Hope National Medical Center

Dan J. Raz (✉ draz@coh.org)

City of Hope National Medical Center

Research

Keywords: NSCLC, Histone methyltransferase G9a, Invasion, Focal adhesion kinase (FAK), Nuclearfactor-kappa B (NF-kB)

Posted Date: June 17th, 2020

DOI: <https://doi.org/10.21203/rs.3.rs-35579/v1>

License: © ⓘ This work is licensed under a Creative Commons Attribution 4.0 International License.

[Read Full License](#)

Abstract

Background

Overexpression of euchromatic histone methyltransferase 2 (EHMT2 or G9a) is frequently found in a number of human cancers. Potential roles of G9a in invasion and metastasis are not well understood in non-small cell lung cancer (NSCLC). Here we investigated the effect and underlying mechanisms of G9a, and therapeutic implications of targeting G9a in the invasion of NSCLC.

Methods

G9a-associated gene sets were identified by RNAseq analysis. Migration and invasion assays were applied to examine the impact of targeting G9a by siRNA knockdown or its specific inhibitor UNC0638 in NSCLC cells. Rescue experiments were designed to investigate the effect of focal adhesion kinase (FAK) and NF- κ B inhibitors on the invasion of NSCLC cells overexpressing G9a. Correlation between the protein level of phosphorylated FAK and G9a was analyzed in NSCLC tissues.

Results

Knockdown and inhibition of G9a drastically suppressed in vitro cellular proliferation, migration, and invasion; while overexpression of G9a significantly enhanced proliferation, migration, and invasion of A549 and H1299 NSCLC cells. Targeting G9a led to a significant decrease in the expression of FAK protein and activation of FAK signaling pathway in both A549 and H1299 cells. Additionally, defactinib, a potent FAK inhibitor, partially abolished the enhanced migration and invasion by overexpression of G9a in these NSCLC cells. Furthermore, G9a was found to boost nuclear factor-kappa B (NF- κ B) transcriptional activity in NSCLC cells through partially downregulating inhibitor of κ B ($I\kappa$ B α), and an NF- κ B inhibitor partially abolished the enhanced FAK activation by overexpressed G9a, which suggests that G9a-enhanced invasion and activation of FAK may be mediated by elevated NF- κ B activity. Notably, a strong positive correlation between the immunohistochemical staining of G9a and phosphorylated FAK proteins was identified in H1299 xenografts and 159 cases of NSCLC tissues ($R = 0.408$).

Conclusions

These data strongly demonstrate that G9a may promote invasion and metastasis of NSCLC cells by enhancing FAK signaling pathway via elevating NF- κ B transcriptional activity, indicating potential significance and therapeutic implications of these pathways in the invasion and metastasis of NSCLCs that overexpress G9a protein.

Background

Lung cancer is a major global health problem and is the leading cause of cancer-related mortality in both men and women[1]. Although advances including lung cancer screening, targeted therapies, and immunotherapy have improved outcomes in patients with lung cancer[2], the overall 5-year survival of

lung cancer patients is still just 5% for patients with advanced lung cancer[3]. Therefore, novel therapeutic approaches for lung cancer are urgently needed.

As a histone methyltransferase encoded by the euchromatic histone-lysine N-methyltransferase 2 (EHMT2), G9a is responsible for catalyzing mono-methylation and di-methylation of Histone H3 Lysine 9 (H3K9me1 and H3K9me2), and plays an important role in regulating gene expression[4]. G9a epigenetically blocks tumor suppressors and activates oncogenes leading to carcinogenesis and cancer cell growth. Previous studies have shown that G9a expression is elevated in many types of human cancers, including lung, breast, colorectal, pancreatic, and bladder cancers[5-7]. Overexpression of G9a is associated with enhanced proliferation and metastasis in many cancer types. However, the underlying mechanisms about how G9a participates in lung cancer metastasis are still poorly understood.

Tumor metastasis is the major cause of cancer-related death, yet precise mechanisms of metastasis remain incompletely understood[8]. Focal Adhesion Kinase (FAK) has been shown to play a central role in metastasis. FAK is a non-receptor cytoplasmic tyrosine kinase which is transcriptionally regulated by P53 and NF- κ B[9]. It contributes to almost every aspect of tumor metastasis, as well as cancer cell adhesion, growth, migration and invasion [10, 11]. Enhanced phosphorylation of FAK at specific sites, especially at Y397, has been reported in a number of cancer types[12]. Studies have shown that FAK is up-regulated in non-small cell lung cancers (NSCLC)[13] and is associated with an aggressive clinical course [14]. In patients with KRAS mutation, FAK is a potential druggable target as it is a downstream effector of KRAS signaling[15]. In KRAS-driven lung adenocarcinomas, FAK inhibitors showed potent antitumor effects in KRAS-G12V-INK4a/ARF-deficient lung cancers in mice[16]. Preclinical data in KRAS-mutated lung cancers showed that inhibition of FAK resulted in sustained DNA damage by suppressing DNA repair mechanisms and enhancing radiation sensitivity [17]. In addition, FAK is considered to be a potential therapeutic target to prevent tumor metastasis in a number of solid tumors[18].

Recently, we reported that G9a was frequently overexpressed in NSCLC tissues and that targeting G9a potently suppressed the growth of NSCLC cells, suggesting that G9a may be a therapeutic target for NSCLC[19]. In this study, we extended our investigation into the role of G9a in NSCLC cellular migration, invasion, and metastasis. We studied potential mechanisms of G9a-mediated invasion and its impact on FAK signaling pathway in NSCLC. Additionally, we explored the effect of targeting G9a on invasive potential and the activation of FAK signaling pathway in NSCLC cells.

Materials And Methods

Cultured cell lines and treated inhibitors

Two human RAS mutated non-small cell lung adenocarcinoma cell lines were used in this study. Both cell lines were purchased from American Type Culture Collection (ATCC, USA). H1299 was cultured in RPMI 1640 (ATCC, USA) medium and A549 was cultured with DMEM/F12 (Corning, USA) medium. For all cell lines, growth medium was supplemented with 10% FBS, 100 U/mL penicillin and 100 mg/mL streptomycin. UNC0638, a selective inhibitor for G9a and GLP methyltransferase, was purchased from

Cayman Chemical Company (USA) and used at a concentration of 2.5 μM and 5 μM . Defactinib hydrochloride, a FAK inhibitor which inhibits FAK phosphorylation at Tyr397, was purchased from MedChemExpress (USA) and used at a concentration of 1 μM . Parthenilide, NF- κB inhibitor, was purchased from Abcam and used at a concentration of 20 μM .

Plasmids, Cell transfection, and qRT-PCR

G9a mRNA (isoform a) was cloned into pcDNA3.1 vector with Hind III and EcoR I (New England BioLabs, USA). Two independent G9a siRNAs: Cat No.10630318 (5'-GGCAUCUCAGGAGGAUGCCAAUGAA-3') and Cat No. 10620319 (5'-UUCAUUGGCAUCCUCCUGAGAUGCC-3') purchased from Thermo Fisher Scientific Corporation (Carlsbad, USA) were used to silence G9a expression by using RNAi maxi reagent (Invitrogen, USA) as describe previously [20]. Cells were transfected with G9a-pcDNA3.1 plasmid and pcDNA3.1 plasmid as control by using Lipofectamine 3000 reagent (Invitrogen, USA) according to the manufacturer's protocol. Total RNAs from cells were extracted with RNeasy Mini Kit (Cat#: 74104) and cDNA was synthesized from 1.0 μg RNA with QuantiTech[®] Reverse Transcription Kit (Cat#:205313) which were purchased from Qiagen Company. G9a (Forward: GGACATCATCACTCATGCGGAAA, Reverse: GCAAAACCATGTCCAAACCAGG), FAK (Forward: GCAATGGAGCGAGTATTAAAGGTC, Reverse: TGGCCACATGCTTTACTTTGTGAC) and GAPDH (Forward: GGGAAAGGTGAAGGTCCGAGTC, Reverse: GAGTTAAAAGCAGCCCTGGTGAC) primers were used in the qRT-PCR assay to quantitatively measure the mRNA expression. Power SYBR[®] Green PCR Master Mix was purchased from Life Technology LTD (Cat#: 4367695). Data was presented as ratio to control to show the relative expression of target, normalized to internal control and relative to the calibration sample.

Cell proliferation, Migration and Invasion Assays

For cell proliferation, cells were seeded as 1×10^5 per well in 6 well plates. After 72 hours, cells were harvested and counted with Cello-meter Spectrum (Nexcelom Bioscience, USA). For migration assay, after transfected with siRNA, plasmids or treated with inhibitors for 48 hours, cells were detached from tissue culture plate by using 0.25% Trypsin-EDTA solution, and pelleted by centrifugation. The cells were resuspended in serum free culture medium and seeded as 5×10^5 per well in a 6-well plate. After 24 hours, cells were scratched with the tip of 20ul pipette and washed twice with PBS. Cells were then cultured with serum free medium and treated with inhibitors. Images were captured immediately after scratching (0 hour), and then at 24h for H1299 and 36h for A549. Five locations were imaged for each well. Migration distances were measured by image J software. Three measurements were performed for each image and average migratory distance was determined. Cell invasion assay was performed using 8 μm Matrigel invasion chambers (Corning, USA). Cells were detached after being transfected or treated with inhibitors for 48 hours as previously described [21]. Then 2.5×10^4 cells were seeded on top of the insert with serum-free medium. Lower chambers were filled with growth medium with 10% FBS. The culture medium was continuously supplemented with respective inhibitor in the inhibitors treated group. After 22 hours, media containing the remaining cells that did not migrate from the top of the membrane was carefully removed. Cells were fixed by placing the insert in 500 μl 10% formalin for 15 min, air-drying for 10 min at room

temperature, and staining with 1% crystal violet solution for 10 minutes. The fixed inserts were then washed with distilled water. Trans-wells were imaged by microscope and cells were counted using Qu path software[22]. Data were analyzed and presented as the ratio of the average of total number in treated group divided by the average of total number in the paired control group.

Western Blot

Total cellular protein samples were extracted with SDS lysis buffer and heated in 95°C for 7 minutes. Proteins were separated by electrophoresis and transferred onto Polyvinylidene fluoride (PVDF) membranes (Thermo Fisher, USA). Membrane was blocked with 5% nonfat milk in PBST for 40min in room temperature and blotted with primary and secondary antibodies, respectively. A primary antibody against β -actin (1:3000) was purchased from Santa Cruz Biotechnology. FAK (1:1000), pFAK (Tyr397) (1:1000), I κ B α (1:1500), H3K9-me2 (1:2000) antibodies were purchased from Cell Signaling Technology. Antibody against G9a (1:1000) was purchased from GeneTex Inc (USA).

Luciferase Reporter Assay of NF- κ B

pSI-Check2-hRLuc-NF κ B-firefly was a gift from Qing Deng (Addgene plasmid # 106979; <http://n2t.net/addgene:106979>; RRID:Addgene_106979) [23]. For each well, 50 ng NF- κ B reporter plasmids were transfected into cells at a concentration of 3×10^3 per well for H1299 and 5×10^3 per well for A549 in 96-well plates using lipofectamine 3000 reagent, with either siRNAs or the overexpression plasmids. For inhibitor experiments, cells were treated with UNC0638 12 hours after transfection with the NF- κ B plasmid. At 72 hours post transfection, cells were washed with PBS and lysed with 40 μ l 1 \times passive lysis buffer. *Firefly* and *renilla* luciferase activity were detected by using Dual-Luciferase[®] Reporter Assay System (Promega, USA). For each group, five replicate experiments were performed. *Firefly* and *renilla* luciferase activities were determined and calculated as described previously (24).

In vivo Xenograft Model

All animal protocols were approved by the institutional animal care and use committee (IACUC, 16005) of City of Hope and performed in the animal facility at City of Hope in accordance with federal, local, and institutional guidelines. H1299 cell line was transfected with G9a-shRNA-GFP plasmid and transfected cells were selected with puromycin. NOD/SCID/IL2R gamma null mice (NSG, 24-27g, 8-10 weeks of age, 6 mice per group) from Jackson Labs (Bar Harbor, USA) were used for xenograft experiment. A suspension of 5×10^6 tumor cells (H1299 shRNA-control and H1299 G9a-shRNA) in 0.1 ml RPMI 1640 was injected into the subcutaneous dorsa of mice at the proximal midline [25]. About 3 weeks after injection, mice were euthanized by CO₂ inhalation, and tumors were excised and fixed for IHC staining.

Immunohistochemistry Analysis

This study was reviewed and approved by the Institutional Review Board (IRB, 13240) of City of Hope National Medical Center. All subjects gave written informed consent. A total of 250 patients with lung

adenocarcinoma and squamous carcinoma who underwent surgical resection for curative intent between 2002 and 2014 without preoperative chemotherapy or radiation therapy were included, as previously reported [19]. Formaldehyde-fixed paraffin embedded (FFPE) tumor samples were sectioned and stained for G9a, H3K9me2 and pFAK (Tyr397) at the pathology core laboratory, as previously described [26]. Antibody against pFAK (Tyr397) (1:2000) was purchased from Invitrogen (Cat#: 700255). Antibody against G9a (1:300) was purchased from GeneTex (Cat#: 129153). Antibody against H3K9me2 (1:200) was purchased from Abcam (Cat#: 5327). G9a and pFAK (Tyr397) IHC staining was scored according to different expression positive percentage and intensity as 0 negative, +minimal, ++ moderate and +++ strong, as we reported previously.

Results

G9a regulates PTK2 gene expression in NSCLC cells

Through gene expression profiling by RNA-Seq analysis, of which the original data is saved on NCBI GEO website with accession number GSE113493, and gene set enrichment analysis, we found that knockdown of G9a significantly suppressed gene sets of cell motility and cell adhesion signaling pathways of NSCLC cells, which are critical for cancer invasion and metastasis; notably, PTK2 that encodes FAK protein is among these significantly downregulated genes in the gene sets, suggesting that PTK2 may represent an important G9a target [19]. To further validate the finding and explore the association between G9a and FAK expression, we first knocked down G9a in H1299 and A549 cells with two independent siRNAs. qRT-PCR showed that G9a mRNA expression level was significantly silenced in both H1299 and A549 cell lines transfected with specific G9a siRNAs (**Figure 1a**, $P < 0.01$). Simultaneously, mRNA expression of PTK2 gene was down regulated in these two cells (**Figure 1b**, $P < 0.05$). As shown in **Figure 1c**, in both A549 and H1299 cell lines, upon knockdown of G9a, the level of H3K9me2 was decreased, and FAK protein was also dramatically decreased in both H1299 and A549 cell lines. These data indicate that FAK expression is associated with G9a expression in NSCLC.

Knockdown and inhibition of G9a suppresses cell migratory and invasive potential of NSCLC cells

To investigate the potential roles of G9a in cell migration and invasion of NSCLCs, cancer cells were first transfected with two different G9a-specific siRNAs for *in vitro* migration and invasion assays. We observed that cell proliferation was also significantly suppressed ($P < 0.01$) upon G9a knockdown in these two lung cancer cells (**Figure S1a&b**). As shown in **Figure 2a**, compared to the control group, cell migration potential was significantly suppressed upon knockdown of G9a in both H1299 (upper panel) and A549 (lower panel) cell lines. A significantly decreased migration distance ($P < 0.001$) was observed in both H1299 and A549 cells upon G9a knockdown (**Figure 2b**).

Invasion assay was carried out in G9a-silenced cells. As shown in **Figure 2c**, cells transfected with G9a siRNA showed lower invasive potential compared to cell transfected with the control siRNA in both H1299 (upper panel) and A549 (lower panel) cells. Statistics analysis showed that compared to the controls, the invasive potential of the G9a-silenced groups decreased significantly ($P < 0.05$) in the two NSCLC cells

(**Figure 2d**). To examine if pharmacological inhibition on G9a activity will also suppress the invasive potential of lung cancer, UNC0638, a selected G9a inhibitor, was used to suppress the G9a methyltransferase activity. As shown in **Figure 2e**, a drastically decrease of H3K9me2 protein was found in cancer cells treated with UNC0638, indicating the methyltransferase activity of G9a was inhibited significantly. Similar to the data of G9a knockdown experiment, cell migration in these two cells was also suppressed by UNC0638 treatment (**Figure S2a**). Compared to the control group, a significant decrease was observed in UNC0638 treated cells (**Figure 2f, left panel**) in these two cells ($P < 0.05$). Besides, the number of invasive cells in A549 and H1299 cell lines was also significantly decreased by UNC0638 treatment (**Figure S2b**). Quantitative analysis of invasive data was presented in **Figure 2f, right panel** ($P < 0.05$). Therefore, above data suggests G9a plays an important role in migratory and invasive potential of NSCLC cell lines.

Inhibition of G9a suppresses the activation of FAK signal pathway in NSCLC

Considering the critical role of FAK in cancer migration and invasion, we hypothesize that G9a may regulate cell invasion and migration through FAK signal pathway. To investigate this underlying mechanism, total protein was extracted from cells either transfected with G9a siRNA or treated with UNC0638. Western blot analysis showed that, compared to control siRNA group, FAK and phosphorylation of FAK (**Figure 3a**) were drastically decreased in both A549 and H1299 cells upon G9a knockdown. Similarly, after being treated with UNC0638 for 72 hours, total FAK and phospho-FAK (pFAK at Tyr397, an autophosphorylation site on the activated FAK that is used as an indicator for FAK activation) proteins were decreased in the both two cell lines (**Figure 3b**). In contrast, overexpression of G9a significantly elevated the levels of FAK and pFAK (Tyr397) (**Figure 3c**). These data indicated that G9a positively regulates the expression of PTK2 gene and activation of FAK signal pathway in NSCLC cells.

Overexpression of G9a enhances cell migratory and invasive potential of NSCLC cells

To further validate the role of G9a in migration, invasion and activation of FAK signal pathway of NSCLC cells, we inserted G9a gene into the pcDNA3.1 vector (**Figure S2**) and examined if G9a overexpression will enhance the invasion and activation of FAK signaling pathway. Consistently, compared to control cells, we observed overexpression of G9a significantly increased lung cancer cell proliferation (**Figure 4Sa&b**, $P < 0.05$). Meanwhile, migration of NSCLC cells (**Figure 4a**) was significantly increased with overexpressed G9a protein ($P < 0.001$, **Figure 4b&c**). Furthermore, compared to control group, the invasion of NSCLC cells was also increased significantly with overexpression of G9a protein (**Figure d&e**, $P < 0.05$). These data further demonstrated a key role of G9a in cell invasion, migration as well as activation of FAK signal pathway in NSCLC.

G9a regulates cell migration and invasion through FAK signal pathway

To investigate whether G9a promotes cell invasion and migration directly or indirectly through activating FAK signal pathway, a rescue experiment was designed. In this experiment we investigate if the FAK inhibitor (defactinib) can suppress the G9a enhanced FAK activation and cell invasion in NSCLC cells. As

shown in **Figure 5a**, overexpression of G9a enhanced the phosphorylation of FAK, while FAK inhibitor defactinib attenuated or even completely abolished the elevated phosphorylated FAK. While cell migration (**Figure 5b&c**) and invasion (**Figure 5d&e**) were boosted by overexpression of G9a, similar to the change in phosphorylated FAK, the enhanced migration and invasion was reversed by FAK inhibitor in these two cell lines. Therefore, the above data suggests that the elevated cell invasion by overexpression of G9a was partially abolished by FAK inhibitor, and G9a promoted cell invasion and migration via activating of FAK signal pathway.

G9a activates FAK signal pathway by elevating NF- κ B transcriptional activity

Studies have already demonstrated that FAK was transcriptionally regulated by P53 and NF- κ B transcription factors (9). We observed the regulation of FAK expression by G9a in both p53-wildtype A549 and p53-null H1299 cells, therefore, we hypothesized that G9a might activate FAK expression through NF- κ B signaling pathway. Therefore, we investigated the effect of knockdown and overexpression of G9a on transcriptional activity of the NF- κ B-controlled luciferase reporter. Dual-luciferase assays showed that silencing of G9a significantly suppressed NF- κ B luciferase activity (**Figure 6a**, $P < 0.05$), while overexpression of G9a significantly increased NF- κ B activity (**Figure 6b**, $P < 0.01$) in these two NSCLC cell lines. UNC0638 also significantly suppressed NF- κ B luciferase activity in both the cell lines (**Figure 6c**, $P < 0.05$). Interestingly, the level of I κ B α protein, an inhibitor of NF- κ B signaling pathway, was found to be upregulated by knockdown of G9a and downregulated by overexpression of G9a (**Figure 6d**), indicating that suppression of G9a on I κ B α expression may contribute to the over-activation of NF- κ B signaling pathway.

To further investigate whether G9a activates FAK signal pathway through NF- κ B, we treated the G9a-overexpressed H1299 cells with a NF- κ B inhibitor, Parthenolide. Western blot analysis showed that NF- κ B inhibitor could partially abolish the elevated phosphorylation of FAK (Tyr397) that was caused by overexpression of G9a (**Figure 6e**). Taken together, these data indicate that G9a activates FAK signal pathway partially through NF- κ B signal pathway.

pFAK (Tyr397) level is correlated with G9a *in vivo* and in NSCLC tissues.

We further investigated the correlation between G9a expression and FAK activation in xenografts using stable G9a-KD H1299 cells. As shown in **Figure 7a**, tumor tissue was stained with H&E staining. Compared to the xenograft tissues of the controls, the IHC intensities of G9a and H3K9me2 were strongly decreased in G9a-attenuated xenograft tissues. Consistent with the *in vitro* data, pFAK (Tyr397) levels were down-regulated dramatically in G9a-attenuated xenograft tissues, suggesting the activation of FAK signaling pathway was suppressed.

Furthermore, we analyzed the correlation between G9a and FAK expression after IHC staining of pFAK (Tyr397). IHC analysis demonstrated nuclear G9a staining (**Figure 7b**), and quantitative analysis of G9a on IHC slides was conducted as previously reported (19). IHC analysis showed cytoplasmic pFAK (Tyr397) staining in tumors and staining was absent in adjacent normal cells. pFAK (Tyr397) IHC staining

in the same tissue arrays were quantitatively scored using the same scoring method, and representative images of IHC scoring are shown in **Figure 7c**. Pearson correlation analysis was used to examine the correlation between G9a and pFAK (Tyr397) IHC staining in these tumor tissues, and the analysis revealed that pFAK (Tyr397) staining was significantly correlated with G9a staining (**Figure 7d**; $R = 0.408$, $P < 0.001$), indicating overexpression of G9a may enhance activation of FAK signaling pathway and then invasion and metastasis in NSCLC.

Discussion

This study demonstrated for the first time that G9a may promote migration and invasion of NSCLC by activating FAK signaling pathway. Our data suggest that in NSCLC, G9a inhibits I κ B α protein to activate NF- κ B, which in turn promotes FAK expression, promoting cell migration and invasion. Given the important role of both G9a and FAK in cancer cell growth and metastasis, this study underscores the potential role of G9a inhibition as a therapeutic target for lung cancer.

With knockdown of G9a or inhibition of G9a methyltransferase activity, cell migration and invasion were inhibited while FAK and phosphorylation of FAK (Tyr397) were downregulated in lung cancer cells. Through rescue experiments, we confirmed that G9a promotes cell growth, migration and invasion by activating FAK signaling. Functionally, G9a is responsible for mono or di-methylation of H3K9 and its activity leads to silencing of a number of tumor suppressor genes including P53, CDH1, DUSP5 and SPRY4 [27, 28]. G9a expression is associated with poor prognosis. For example, G9a promotes cancer invasion and metastasis by silencing Ep-CAM in lung cancer [29]. Additionally, it is considered a marker of aggressive ovarian cancer and correlated with peritoneal metastasis [30]. It is also responsible for liver cancer development and metastasis by silencing tumor suppressor RARRES2 [31]. Recently, G9a has been demonstrated to promote tumor metastasis by upregulating ITGB3 in gastric cancer [32]. G9a is also involved in hypoxia-induced epigenetic regulation in ovarian cancer [33]. Furthermore, G9a is known to activate hypoxia signaling pathway leading to suppression of apoptosis. Under normoxia, G9a is hydroxylated and inhibited by factor inhibiting HIF (FIH). However, under hypoxia, it is associated with hypoxia induced signal pathway in angiogenesis, including MMP2, VEGFR-2 and FAK in HUVECs [34]. G9a was also found to suppress hypoxia-dependent gene type-II cadherin CDH10, which leads to advanced cellular movements in breast cancer cell lines [35].

In addition, G9a expression is closely associated with tumorigenesis, metastasis and drug resistance in many cancers [36]. We previously reported that G9a promotes tumor growth via enhancing HP1 α and silencing APC2 expression (19). Researchers have shown that G9a is transcriptionally regulated by special AT-rich sequence-binding protein 2 (SATB2). Decreased expression of SATB2 leads to increased invasiveness of NSCLC through upregulation of G9a expression [37]. G9a expression in endometrial cancer is negatively correlated with E-cadherin expression and enhanced the depth of myometrial invasion [38]. Others have reported that the G9a inhibitor UNC0638 reduced growth and metastasis of breast cancer and also significantly suppressed epithelial-mesenchymal transition-mediated cellular migration and invasion [39]. Another G9a methyltransferase activity inhibitor, UNC0646, was shown to

suppress hepatocellular tumor growth but activate cellular apoptosis and metastasis [40]. Although G9a inhibitors hold promise as a therapy for solid tumors, none have successfully been advanced to clinical trials.

Meanwhile, we have found that FAK signaling pathway is a downstream target of G9a. FAK plays a pivotal role in transducing signals from the plasma membrane to the nucleus, and phosphorylation of FAK promotes cancer cell growth, invasion, and angiogenesis [41]. High expression of pFAK (Tyr397) is associated with aggressive behavior of lung cancer, including rapid growth, frequent metastasis and poor overall survival [42]. A phase I study of the FAK inhibitor BI 853520 showed that FAK inhibitor produced promising results in patients with advanced or metastatic solid tumor [43]. Several other phase I and phase II clinical trials are currently undergoing for FAK inhibitors in cancer [44]. FAK could be a potential combination therapy target for patients with G9a overexpressing lung cancers.

In addition, this study demonstrated for the first time that G9a regulates FAK through NF- κ B signaling pathway. NF- κ B is activated by various stimuli, including hypoxia, cytokines (including TNF- α and IL-1 β), growth factors, and DNA damage in tumor tissues. These stimuli lead to the activation of the inhibitor of κ B (I κ B α) kinase (IKK) complex. The activated IKK complex promotes the phosphorylation of I κ B α and its degradation. I κ B α forms a complex with P50 and P65. With the degradation of I κ B α , P50 and P65 translocate to the nucleus to regulate downstream gene expression [45]. Previous study reported an association between G9a activity and NF- κ B signaling [46]. In our study, we revealed that elevated expression of G9a suppressed I κ B α protein and increased NF- κ B luciferase activity, activating FAK signaling and promoting migration and invasion in NSCLCs. Similarly, recent study has demonstrated that NF- κ B signaling pathway plays a very important role in oncogenesis and metastasis [47]. NF- κ B signaling pathway has previously been shown to be associated with FAK activation and increased cell proliferation in lung cancer [48]. Tetraspanin 15 (TSPAN15) promoted esophageal cancer metastasis via activating NF- κ B through regulating I κ B α phosphorylation [49]. In NSCLC, researchers have found that HMGB1 mediated cancer cell motility is mediated in part by NF- κ B-activated FAK signaling pathway [50]. These and other studies demonstrate the important role of NF- κ B in FAK signaling pathway and cancer metastasis and suggest that NF- κ B can also be considered as a potential druggable target in patients with G9a overexpressing lung cancers.

Conclusions

In summary, we have revealed a novel mechanism by which G9a mediates invasion and metastasis in NSCLC. We have demonstrated that the role of G9a in lung cancer invasion and metastasis is mediated in part by enhanced activation of FAK that appears to be mediated by NF- κ B (**Figure 7e**). These findings suggest that the interaction between G9a, FAK, and NF- κ B may be druggable targets for NSCLC that overexpress G9a.

Data Analysis

All experiments were performed in duplicates or triplicates and repeated at least two times. For group-group statistics analysis, data were analyzed for variation and significance using Student's T test. All data are shown as mean \pm SD. Statistical significance was set at $P < 0.05$. Pearson's correlation coefficient was used to measure correlation of G9a and pFAK (Tyr397) gene expression.

List Of Abbreviations

G9a, Euchromatic histone-lysine N-methyltransferase 2 (EHMT2); FAK, *focal adhesion kinase*; NF- κ B, Nuclear Factor kappa-light-chain-enhancer of activated B cells; NSCLC, non-small cell lung cancer; H3K9me2, di-methylation at the 9th lysine residue of the histone H3 protein; Ep-CAM, *Epithelial cell adhesion molecule*; qRT-PCR, quantitative reverse transcription polymerase chain reaction; CDH1, cadherin 1; DUSP5, Dual-specificity phosphatase 5;SPRY4, sprout RTK Signaling Antagonist 4;RARRES2, Retinoic Acid Receptor Responder 2; ITGB3, Integrin beta-3; KRAS, Kirsten rat sarcoma 2 viral oncogene homolog; ATCC, American Type Culture Collection; GLP, G9a-like protein; pFAK, phosphorylation of FAK; I κ B α , inhibitor of κ B α ; IKK, I κ B kinase. HIF, hypoxia induced factor; MMP2, matrix metalloproteinase 2; VEGF-2, vascular endothelial growth factor C; HUVECs, human umbilical vein endothelial cell; HP1 α , heterochromatin protein 1 α ; APC2, adenomatous polyposis coli protein 2; SATB2, special AT-rich sequence-binding protein 2; HMGB1, high mobility group box 1.

Declarations

Ethic approval and consent to participate

For animal xenograft experiments, all animal protocols were approved by the institutional animal care and use committee (IACUC,16005)of City of Hope and performed in the animal facility at City of Hope in accordance with federal, local, and institutional guidelines. For tissue assay patients' sample collection, this study was reviewed and approved by the Institutional Review Board (IRB,13240) of City of Hope National Medical Center. All subjects gave written informed consent.

Consent for publication

All authors agreed on the publication of this manuscript.

Availability of data and materials

Figure S1-S3 was shown in additional file1.

Competing interests

The authors declare no conflict of interest.

Funding

Research reported in this publication is supported by the V Foundation (DR), the Doris Duke Charitable Foundation (DR) and the National Cancer Institute of the National Institutes of Health (NIH P30CA33572) using several core facilities.

Authors contributions

TS performed experiments and analyzed data, wrote the manuscript. KZ conceived and supervised all the studies; and revised the manuscript. RP and WL provided material and technical support on xenograft experiments. YD provided suggestions on experiments and revision. SC provided technical support on IHC staining. LA did the IHC tissue array scoring. DR conceived the study and revised the manuscript. All authors read and approved the final version of the manuscript.

Acknowledgements

We acknowledge the generous support of the Baum Family Foundation in support of this laboratory. The authors thank Michael Lewallen at the pathology core for IHC staining, and Michael Nelson at the light microscope core for Trans-well imaging and cell counting.

References:

1. Siegel RL, Miller KD, Jemal A. Cancer statistics, 2020. *CA Cancer J Clin.* 2020;70(1):7-30.
2. Herbst RS, Morgensztern D, Boshoff C. The biology and management of non-small cell lung cancer. *Nature.* 2018;553(7689):446-54.
3. Heron M, Anderson RN. Changes in the Leading Cause of Death: Recent Patterns in Heart Disease and Cancer Mortality. *NCHS Data Brief.* 2016(254):1-8.
4. Shinkai Y, Tachibana M. H3K9 methyltransferase G9a and the related molecule GLP. *Genes Dev.* 2011;25(8):781-8.
5. Urrutia G, Salmonson A, Toro-Zapata J, de Assuncao TM, Mathison A, Dusetti N, et al. Combined Targeting of G9a and Checkpoint Kinase 1 Synergistically Inhibits Pancreatic Cancer Cell Growth by Replication Fork Collapse. *Mol Cancer Res.* 2019.
6. Segovia C, San Jose-Eneriz E, Munera-Maravilla E, Martinez-Fernandez M, Garate L, Miranda E, et al. Inhibition of a G9a/DNMT network triggers immune-mediated bladder cancer regression. *Nat Med.* 2019;25(7):1073-81.
7. Wang YF, Zhang J, Su Y, Shen YY, Jiang DX, Hou YY, et al. G9a regulates breast cancer growth by modulating iron homeostasis through the repression of ferroxidase hephaestin. *Nat Commun.* 2017;8(1):274.
8. Chaffer CL, Weinberg RA. A perspective on cancer cell metastasis. *Science.* 2011;331(6024):1559-64.
9. Golubovskaya V, Kaur A, Cance W. Cloning and characterization of the promoter region of human focal adhesion kinase gene: nuclear factor kappa B and p53 binding sites. *Biochim Biophys Acta.* 2004;1678(2-3):111-25.

10. Sulzmaier FJ, Jean C, Schlaepfer DD. FAK in cancer: mechanistic findings and clinical applications. *Nat Rev Cancer*. 2014;14(9):598-610.
11. Shen M, Jiang YZ, Wei Y, Ell B, Sheng X, Esposito M, et al. Tinagl1 Suppresses Triple-Negative Breast Cancer Progression and Metastasis by Simultaneously Inhibiting Integrin/FAK and EGFR Signaling. *Cancer Cell*. 2019;35(1):64-80 e7.
12. Aronsohn MS, Brown HM, Hauptman G, Kornberg LJ. Expression of focal adhesion kinase and phosphorylated focal adhesion kinase in squamous cell carcinoma of the larynx. *Laryngoscope*. 2003;113(11):1944-8.
13. Carelli S, Zadra G, Vaira V, Falleni M, Bottiglieri L, Nosotti M, et al. Up-regulation of focal adhesion kinase in non-small cell lung cancer. *Lung Cancer*. 2006;53(3):263-71.
14. Aboubakar Nana F, Lecocq M, Ladjemi MZ, Detry B, Dupasquier S, Feron O, et al. Therapeutic Potential of Focal Adhesion Kinase Inhibition in Small Cell Lung Cancer. *Mol Cancer Ther*. 2019;18(1):17-27.
15. Matikas A, Mistriotis D, Georgoulas V, Kotsakis A. Targeting KRAS mutated non-small cell lung cancer: A history of failures and a future of hope for a diverse entity. *Crit Rev Oncol Hematol*. 2017;110:1-12.
16. Konstantinidou G, Ramadori G, Torti F, Kangasniemi K, Ramirez RE, Cai Y, et al. RHOA-FAK is a required signaling axis for the maintenance of KRAS-driven lung adenocarcinomas. *Cancer Discov*. 2013;3(4):444-57.
17. Tang KJ, Constanzo JD, Venkateswaran N, Melegari M, Ilcheva M, Morales JC, et al. Focal Adhesion Kinase Regulates the DNA Damage Response and Its Inhibition Radiosensitizes Mutant KRAS Lung Cancer. *Clin Cancer Res*. 2016;22(23):5851-63.
18. Wu HJ, Hao M, Yeo SK, Guan JL. FAK signaling in cancer-associated fibroblasts promotes breast cancer cell migration and metastasis by exosomal miRNAs-mediated intercellular communication. *Oncogene*. 2020;39(12):2539-49.
19. Zhang K, Wang J, Yang L, Yuan YC, Tong TR, Wu J, et al. Targeting histone methyltransferase G9a inhibits growth and Wnt signaling pathway by epigenetically regulating HP1alpha and APC2 gene expression in non-small cell lung cancer. *Mol Cancer*. 2018;17(1):153.
20. Zhang K, Gao H, Wu X, Wang J, Zhou W, Sun G, et al. Frequent overexpression of HMGA2 in human atypical teratoid/rhabdoid tumor and its correlation with let-7a3/let-7b miRNA. *Clin Cancer Res*. 2014;20(5):1179-89.
21. Zhang K, Wang J, Wang J, Luh F, Liu X, Yang L, et al. LKB1 deficiency promotes proliferation and invasion of glioblastoma through activation of mTOR and focal adhesion kinase signaling pathways. *American journal of cancer research*. 2019;9(8):1650-63.
22. Bankhead P, Loughrey MB, Fernandez JA, Dombrowski Y, McArt DG, Dunne PD, et al. QuPath: Open source software for digital pathology image analysis. *Sci Rep*. 2017;7(1):16878.
23. Zhou W, Pal AS, Hsu AY, Gurol T, Zhu X, Wirbisky-Hershberger SE, et al. MicroRNA-223 Suppresses the Canonical NF-kappaB Pathway in Basal Keratinocytes to Dampen Neutrophilic Inflammation. *Cell*

- Rep. 2018;22(7):1810-23.
24. Zhang K, Lu J, Mori T, Smith-Powell L, Synold TW, Chen S, et al. Baicalin increases VEGF expression and angiogenesis by activating the ERR α /PGC-1 α pathway. *Cardiovascular research*. 2011;89(2):426-35.
 25. Zhang K, Yang L, Wang J, Sun T, Guo Y, Nelson R, et al. Ubiquitin-specific protease 22 is critical to in vivo angiogenesis, growth and metastasis of non-small cell lung cancer. *Cell Commun Signal*. 2019;17(1):167.
 26. Zhang K, Keymeulen S, Nelson R, Tong TR, Yuan YC, Yun X, et al. Overexpression of Flap Endonuclease 1 Correlates with Enhanced Proliferation and Poor Prognosis of Non-Small-Cell Lung Cancer. *The American journal of pathology*. 2018;188(1):242-51.
 27. Huang J, Dorsey J, Chuikov S, Perez-Burgos L, Zhang X, Jenuwein T, et al. G9a and Glp methylate lysine 373 in the tumor suppressor p53. *J Biol Chem*. 2010;285(13):9636-41.
 28. Wozniak RJ, Klimecki WT, Lau SS, Feinstein Y, Futscher BW. 5-Aza-2'-deoxycytidine-mediated reductions in G9A histone methyltransferase and histone H3 K9 di-methylation levels are linked to tumor suppressor gene reactivation. *Oncogene*. 2007;26(1):77-90.
 29. Chen MW, Hua KT, Kao HJ, Chi CC, Wei LH, Johansson G, et al. H3K9 histone methyltransferase G9a promotes lung cancer invasion and metastasis by silencing the cell adhesion molecule Ep-CAM. *Cancer Res*. 2010;70(20):7830-40.
 30. Hua KT, Wang MY, Chen MW, Wei LH, Chen CK, Ko CH, et al. The H3K9 methyltransferase G9a is a marker of aggressive ovarian cancer that promotes peritoneal metastasis. *Mol Cancer*. 2014;13:189.
 31. Wei L, Chiu DK, Tsang FH, Law CT, Cheng CL, Au SL, et al. Histone methyltransferase G9a promotes liver cancer development by epigenetic silencing of tumor suppressor gene RARRES3. *J Hepatol*. 2017;67(4):758-69.
 32. Hu L, Zang MD, Wang HX, Zhang BG, Wang ZQ, Fan ZY, et al. G9A promotes gastric cancer metastasis by upregulating ITGB3 in a SET domain-independent manner. *Cell Death Dis*. 2018;9(3):278.
 33. Kang J, Shin SH, Yoon H, Huh J, Shin HW, Chun YS, et al. FIH Is an Oxygen Sensor in Ovarian Cancer for G9a/GLP-Driven Epigenetic Regulation of Metastasis-Related Genes. *Cancer Res*. 2018;78(5):1184-99.
 34. Oh SY, Seok JY, Choi YS, Lee SH, Bae JS, Lee YM. The Histone Methyltransferase Inhibitor BIX01294 Inhibits HIF-1 α Stability and Angiogenesis. *Mol Cells*. 2015;38(6):528-34.
 35. Casciello F, Al-Ejeh F, Miranda M, Kelly G, Baxter E, Windloch K, et al. G9a-mediated repression of CDH10 in hypoxia enhances breast tumour cell motility and associates with poor survival outcome. *Theranostics*. 2020;10(10):4515-29.
 36. Liu CW, Hua KT, Li KC, Kao HF, Hong RL, Ko JY, et al. Histone Methyltransferase G9a Drives Chemotherapy Resistance by Regulating the Glutamate-Cysteine Ligase Catalytic Subunit in Head and Neck Squamous Cell Carcinoma. *Mol Cancer Ther*. 2017;16(7):1421-34.

37. Ma YN, Zhang HY, Fei LR, Zhang MY, Wang CC, Luo Y, et al. SATB2 suppresses non-small cell lung cancer invasiveness by G9a. *Clin Exp Med*. 2018;18(1):37-44.
38. Hsiao SM, Chen MW, Chen CA, Chien MH, Hua KT, Hsiao M, et al. The H3K9 Methyltransferase G9a Represses E-cadherin and is Associated with Myometrial Invasion in Endometrial Cancer. *Ann Surg Oncol*. 2015;22 Suppl 3:S1556-65.
39. Liu XR, Zhou LH, Hu JX, Liu LM, Wan HP, Zhang XQ. UNC0638, a G9a inhibitor, suppresses epithelial-mesenchymal transition-mediated cellular migration and invasion in triple negative breast cancer. *Mol Med Rep*. 2018;17(2):2239-44.
40. Gu M, Toh TB, Hooi L, Lim JJ, Zhang X, Chow EK. Nanodiamond-Mediated Delivery of a G9a Inhibitor for Hepatocellular Carcinoma Therapy. *ACS Appl Mater Interfaces*. 2019;11(49):45427-41.
41. Thanappapasr K, Nartthanarung A, Thanappapasr D, Jinawath A. pFAK-Y397 overexpression as both a prognostic and a predictive biomarker for patients with metastatic osteosarcoma. *PLoS One*. 2017;12(8):e0182989.
42. Aboubakar Nana F, Hoton D, Ambroise J, Lecocq M, Vanderputten M, Sibille Y, et al. Increased Expression and Activation of FAK in Small-Cell Lung Cancer Compared to Non-Small-Cell Lung Cancer. *Cancers (Basel)*. 2019;11(10).
43. Doi T, Yang JC, Shitara K, Naito Y, Cheng AL, Sarashina A, et al. Phase I Study of the Focal Adhesion Kinase Inhibitor BI 853520 in Japanese and Taiwanese Patients with Advanced or Metastatic Solid Tumors. *Target Oncol*. 2019;14(1):57-65.
44. Mohanty A, Pharaon RR, Nam A, Salgia S, Kulkarni P, Massarelli E. FAK-targeted and combination therapies for the treatment of cancer: an overview of phase I and II clinical trials. *Expert Opin Investig Drugs*. 2020:1-11.
45. Xia Y, Shen S, Verma IM. NF-kappaB, an active player in human cancers. *Cancer Immunol Res*. 2014;2(9):823-30.
46. Park SE, Yi HJ, Suh N, Park YY, Koh JY, Jeong SY, et al. Inhibition of EHMT2/G9a epigenetically increases the transcription of Beclin-1 via an increase in ROS and activation of NF-kappaB. *Oncotarget*. 2016;7(26):39796-808.
47. Soleimani A, Rahmani F, Ferns GA, Ryzhikov M, Avan A, Hassanian SM. Role of the NF-kappaB signaling pathway in the pathogenesis of colorectal cancer. *Gene*. 2020;726:144132.
48. Xia Y, Yeddula N, Leblanc M, Ke E, Zhang Y, Oldfield E, et al. Reduced cell proliferation by IKK2 depletion in a mouse lung-cancer model. *Nat Cell Biol*. 2012;14(3):257-65.
49. Zhang B, Zhang Z, Li L, Qin YR, Liu H, Jiang C, et al. TSPAN15 interacts with BTRC to promote oesophageal squamous cell carcinoma metastasis via activating NF-kappaB signaling. *Nat Commun*. 2018;9(1):1423.
50. Zhu J, Luo J, Li Y, Jia M, Wang Y, Huang Y, et al. HMGB1 induces human non-small cell lung cancer cell motility by activating integrin alphavbeta3/FAK through TLR4/NF-kappaB signaling pathway. *Biochem Biophys Res Commun*. 2016;480(4):522-7.

Figures

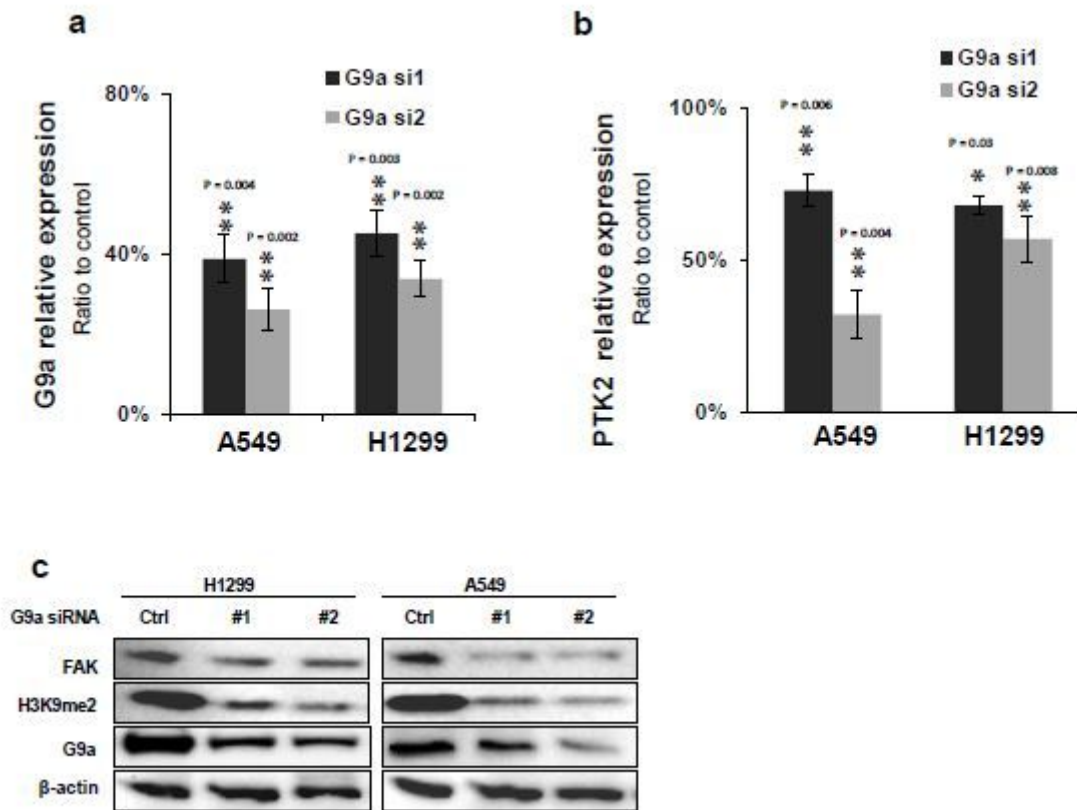


Figure 1

G9a regulates PTK2 gene expression in NSCLC cells. a. qRT-PCR showed that G9a gene expression was down-regulated in NSCLC transfected with G9a siRNAs. Data was presented as the ratio to control (** $P < 0.01$, compared to the controls). b. qRT-PCR showed that PTK2 gene expression was down-regulated upon silence of G9a in NSCLC (** $P < 0.01$). c. Western blot showed that H3K9-Me2 and FAK was downregulated upon silence of G9a in NSCLC. Data are presented as means \pm standard deviation (SD). Three independent experiments were performed.

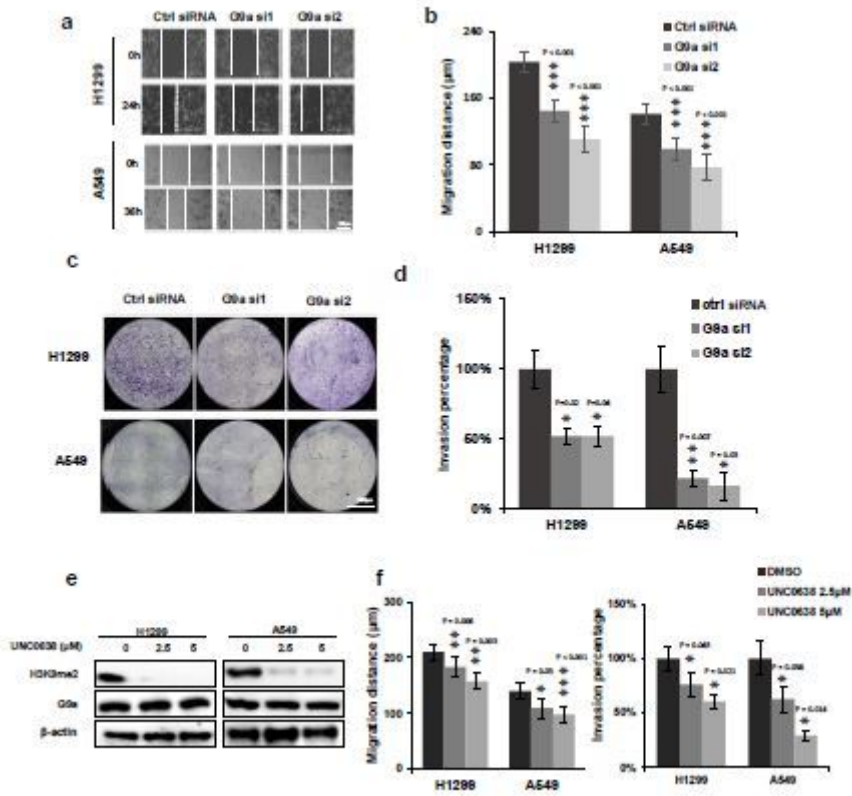


Figure 2

Knockdown and inhibition of G9a suppresses cell migratory and invasive potential of NSCLC cells

a. Representative image of scratch experiments showed that knockdown of G9a suppressed cell migration of NSCLCs. Scale bar refersto 200µm. b. Quantitative analysis of migration distances in G9a-silenced NSCLC cells. ***P < 0.001. c. Representative image of invasive cells showed that knockdown of G9a suppressed cell invasive potential of NSCLCs, scale bar refersto 2000µm. d. Quantitative analysis for invasive cells in G9a-silenced NSCLC cells, *P < 0.05, **P < 0.01. e. Western blots showed that H3K9-Me2 was decreased by G9a inhibitor UNC0638. f. Inhibition of G9a suppressed cell migration and invasion of NSCLC. Left panel: Quantitative analysis of migration distances of H1299 and A549 cells treated with UNC0638. ** p < 0.01. Right panel: Quantitative analysis of invasive cells for H1299 and A549 cell lines treated with UNC0638. Data are presented as the normalized percentage to the control. *P < 0.05, **P < 0.01, ***P < 0.001. Data are presented as means ± standard division (SD). Three independent experiments were performed.

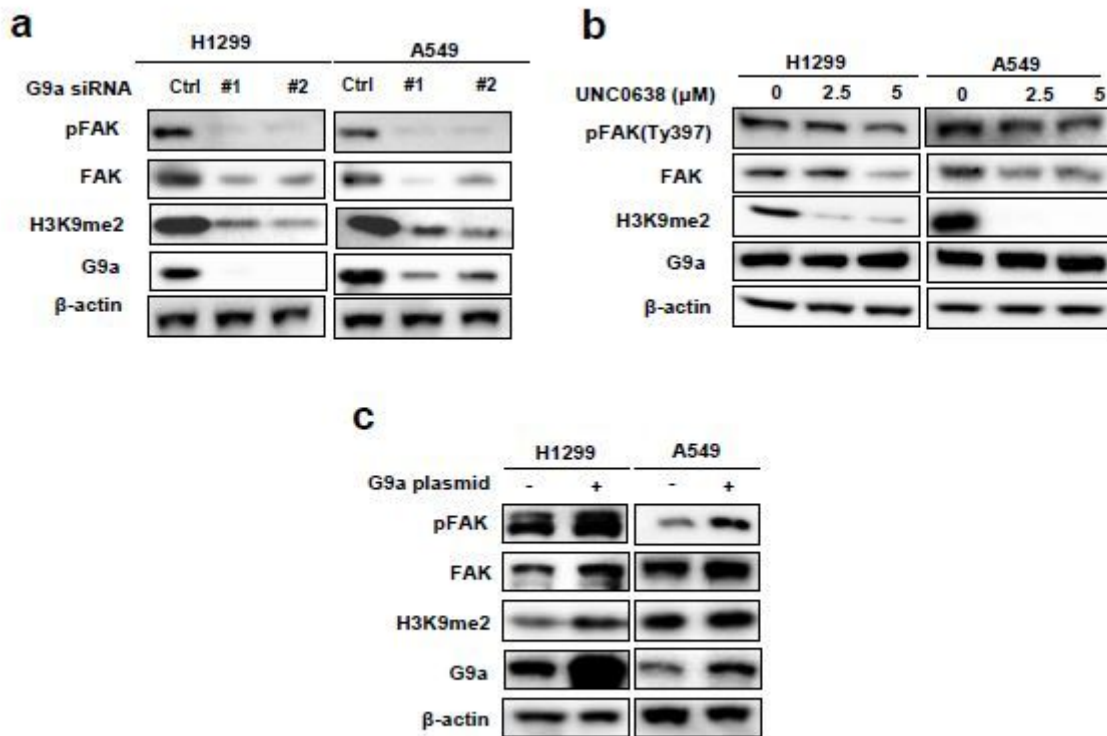


Figure 3

Inhibition of G9a suppresses the activation of FAK signal pathway in NSCLC a. Western blot analysis showing that the total FAK and pFAK (Tyr397) was decreased in G9a-silenced NSCLC cell lines. b. Western blots showing G9a inhibitor UNC0638 decreased the FAK and pFAK (Tyr397) in NSCLC cell lines. c. Western blot analysis showing that overexpression of G9a elevated FAK and pFAK(Tyr397) in NSCLC cell lines. Three independent experiments were performed.

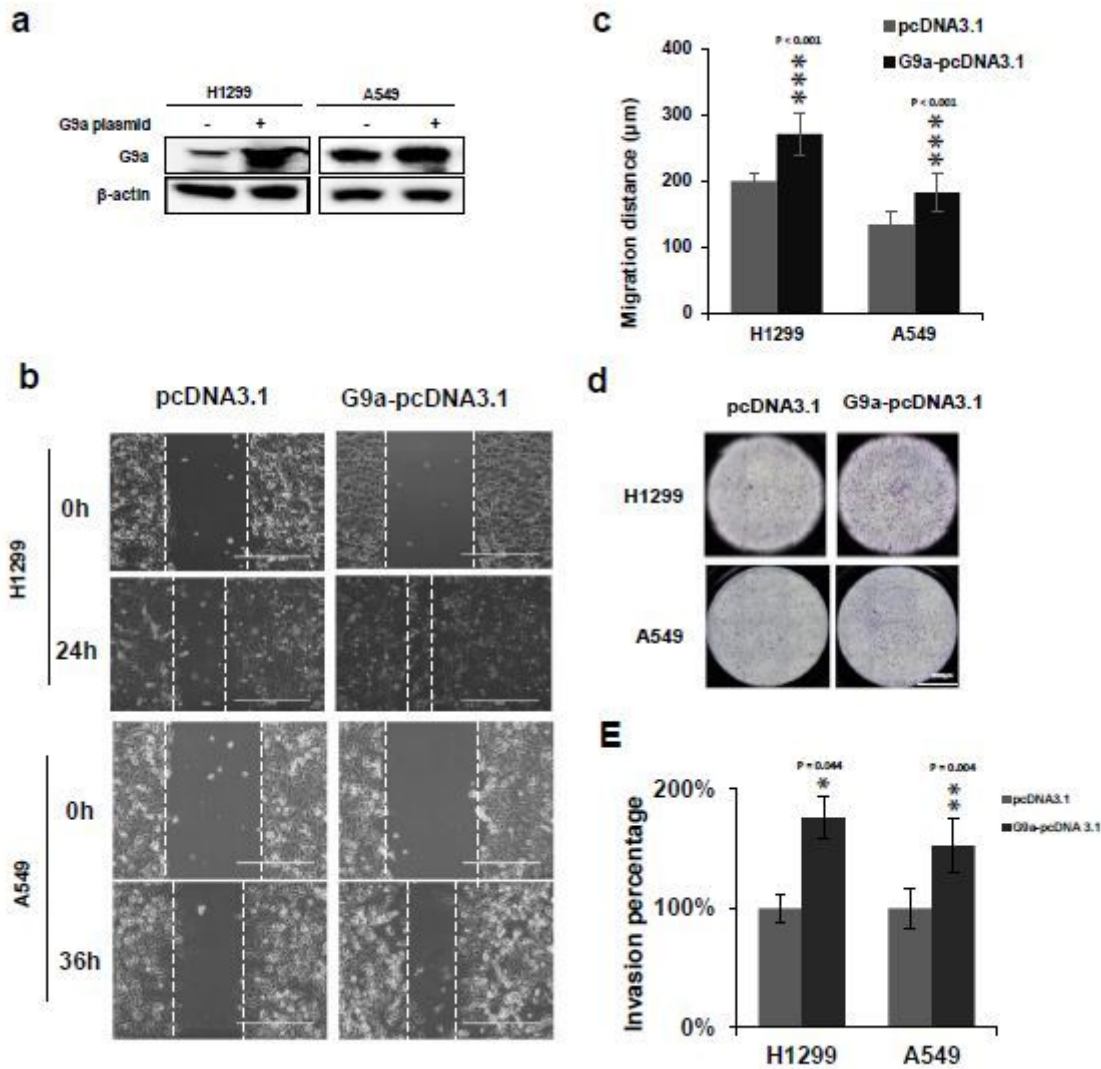


Figure 4

Overexpression of G9a enhances cell migratory and invasive potential of NSCLC cells a. Western blot analysis of G9a overexpression in H1299 and A549 cell lines. b. Representative images of scratch experiments at 0h and 24h for H1299, 0h and 36h for A549 in NSCLC cell lines with overexpressed G9a. Scale bar refersto400μm. c. Representative images of invasive cells in G9a-overexpressed NSCLC cell lines. ***P < 0.001. d. Representative images of invasive cells in G9a-overexpressed NSCLC cell lines. Scale bar refersto2000μm. e. Quantitative analysis for invasive cells in G9a-overexpressed NSCLC cell lines. Data are presented as percentage of control, *P < 0.05, **P < 0.01. Data are presented as means ± standard division (SD). Three independent experiments were performed.

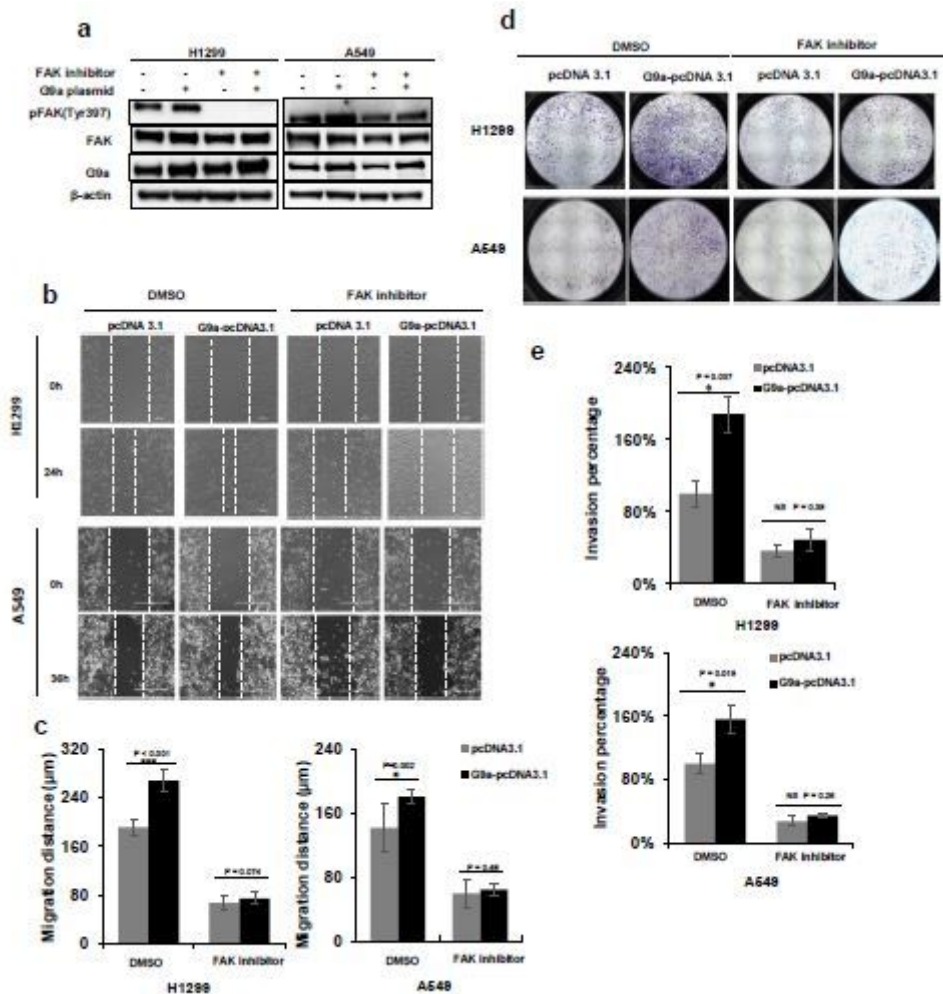


Figure 5

FAK inhibitor attenuates the enhanced cell migration and invasion by G9a overexpression a. Western blots showing that activation of FAK signal pathway was attenuated by FAK inhibitor in G9a overexpressed NSCLC cells. b. Representative images of scratch experiments at 0h and 24h for H1299, 0h and 36h for A549 shows the enhanced migration was reversed by FAK inhibitor in NSCLC cell lines. Scale bar=400μm. c. Quantitative analysis of migration distances in A549 and H1299 cells treated with FAK inhibitor. **P < 0.01, ***P < 0.001, NS, no significant difference. d. The enhanced invasive ability was attenuated by FAK inhibitor in A549 and H1299 cell lines. Representative image of invasive cells in NSCLC cells treated with FAK inhibitor. Scale bar refersto 2000μm. e. Quantitative analysis for invasive cells in G9a-overexpressed A549 and H1299 cancer cells treated with FAK inhibitor. Data are presented as percentage of control, *P < 0.05; NS, no significant difference. Data are presented as means ± standard division (SD). Three independent experiments were performed.

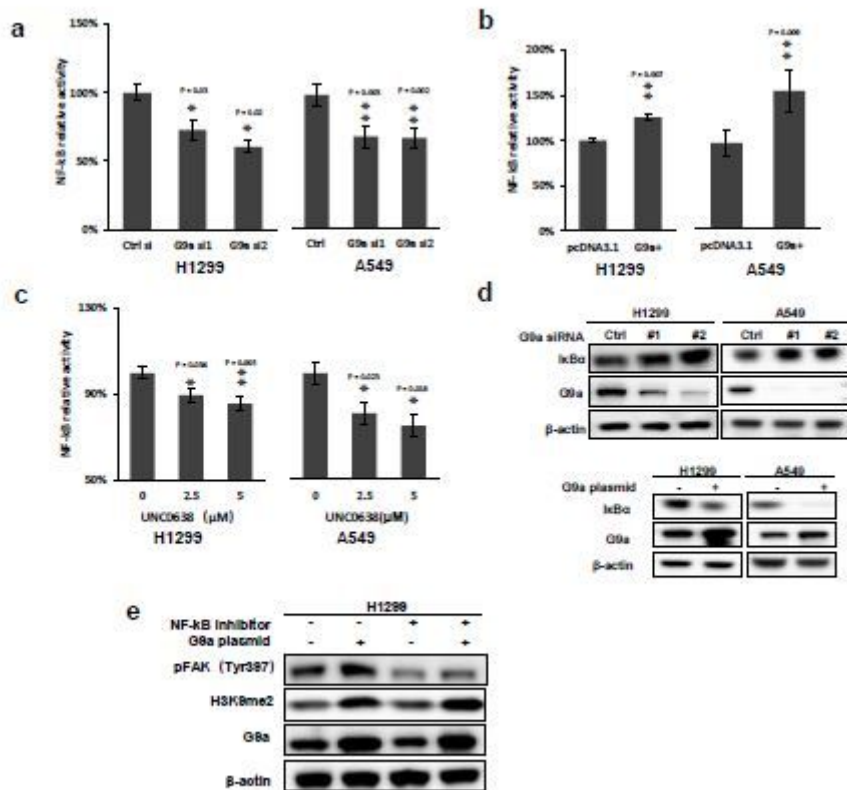


Figure 6

G9a activates FAK signal pathway by elevating NF-κB transcriptional activity a. Knockdown of G9a suppressed NF-κB transcriptional activity in H1299 and A549 cells; *P < 0.05, **P < 0.01 (compared to control siRNA). b. Overexpression of G9a enhanced NF-κB transcriptional activity in A549 and H1299 cells; **P < 0.01 (compared to pcDNA 3.1). c. NF-κB activity was suppressed in UNC0638 treated NSCLCs; *P < 0.05, **P < 0.01 (compared to DMSO treated cell). d. Western blot analysis showed that the expression of IkBα was up-regulated upon overexpression of G9a in A549 and H1299 cells. e. Western blots showed that NF-κB inhibitor partially abolished the elevated phosphorylation of FAK (Tyr397) that was enhanced by overexpression of G9a. All of data are presented as means ± standard deviation (SD). For each group, experiments were performed as triplicates and experiments were repeated three times.

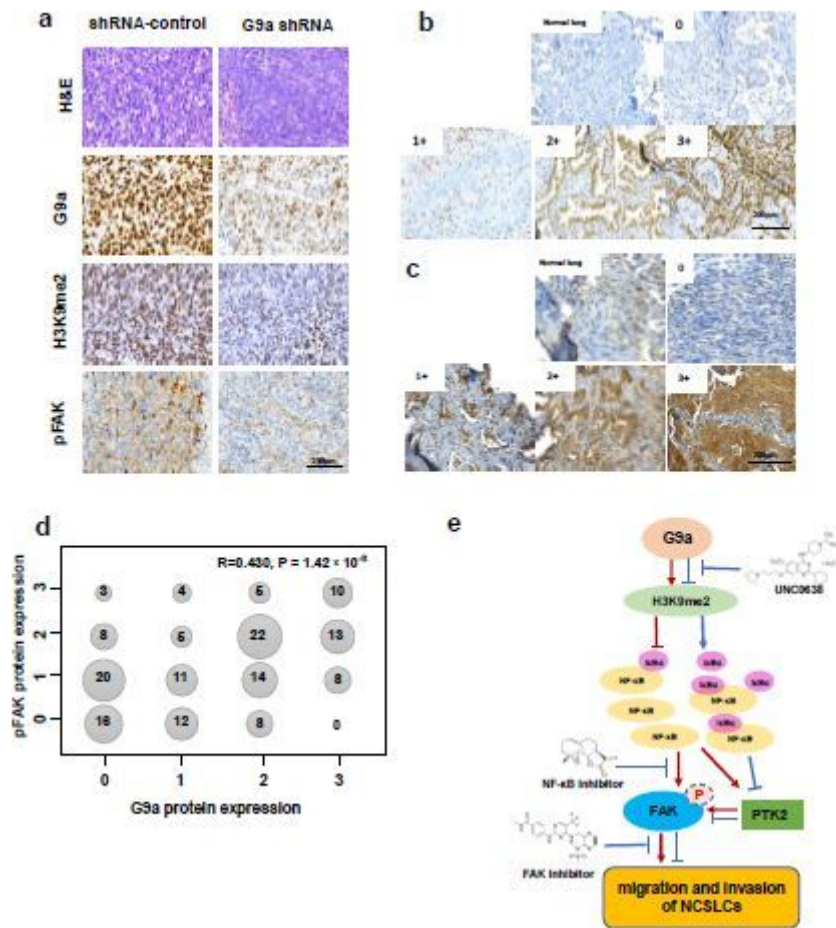


Figure 7

pFAK (Tyr397) level is correlated with G9a in vivo and in NSCLC tissues. a. Representative images of H&E and proteins IHC stained in these xenografts showed that G9a, H3K9me2 and pFAK (Tyr397) were strongly decreased in G9a-attenuated xenograft tissues. Scale bar refersto200µm. b. Representative image scored as 0, 1+, 2+, 3+ for IHC staining of G9a in NSCLC tissue arrays. Scale barrefers to 200µm. c. Representative image scored as 0, 1+, 2+, 3+ for IHC staining of pFAK(Tyr397) G9a in NSCLC tissues. Scale bar refers to 200 µm. d. IHC staining of pFAK (Tyr397) was significantly positively correlated with that of G9a in NSCLC tissues. The numbers in the bubble shows the case for each scored stage. $R = 0.408, p < 0.001$. e. Schematic diagram of the potential mechanisms for G9a-enhanced invasion and related therapeutic implications in NSCLC. G9a di-methylates H3K9, inhibits IκBα expression, thus releases and activates NF-κB signal pathway, finally promotes PTK expression and phosphorylation of FAK at tyrosine 397, eventually promotes NSCLC cell migration and invasion. G9a specific siRNAs and inhibitors down-regulate global H3K9me2 and upregulate IκBα protein, inhibits NF-κB activity, thus suppresses PTK expression and phosphorylation of FAK, eventually suppress migration and invasion of NSCLC. NF-κB inhibitor partially abolished elevated phosphorylation of FAK enhanced by G9a, and FAK inhibitor partially abolished the elevated migratory and invasive potential enhanced by G9a.

Supplementary Files

This is a list of supplementary files associated with this preprint. Click to download.

- [Supplementarymaterials.docx](#)